

## Supporting Information

# Hollow hydroxyapatite nanospheres synthesis by the control of nucleation and growth in a two phase system

Huan Zhao,<sup>a</sup> Yu-Da Zhu,<sup>a</sup> Jing Sun,<sup>a</sup> Dan Wei,<sup>a</sup> Ke-Feng Wang,<sup>a</sup> Ming Liu,<sup>b</sup> Hong-Song Fan\*<sup>a</sup>, and Xing-Dong Zhang<sup>a</sup>

<sup>a</sup> National Engineering Research Center for Biomaterials, Sichuan University, Chengdu, 610064, P. R. China.

<sup>b</sup> Analytical & Testing Center, Sichuan University, Chengdu, 610064, P. R. China.

### 1. Materials and Methods

**Materials:** Calcium (II) stearate, Trisodium phosphate, Lauric acid, Sodium citrate, Sodium borohydride, Gold chloride, Toluene and Dimethyl sulphoxide (DMSO) were purchased from Chengdu Kelong Chemical Reagent Factory, China. Oleic acid (OA) and Oleylamine (OAm) were purchased from TCI, Japan. Bull serum albumin (BSA) was purchased from Beijing Solarbio science & technology Co., Ltd., China. Doxorubicin hydrochloride (DOX, > 99%) were purchased from Beijing Zhongshuo Pharmaceutical Technology Development Co., Ltd., China. Methyl thiazolyltetrazolium (MTT) was purchased from Amreso, USA. Dulbecco's Modified Eagle Medium (DMEM) and fetal bovine serum (FBS) were from Hyclone (USA). All chemicals were analytical grade and used without any further purification. Water was deionized to 18.25 MΩ.CM with a Millipore purification system.

**Typical Method :** In a typical synthesis, 0.0607 g Ca (SA)<sub>2</sub>, 2.0 mL of OA, and 20.0 mL of toluene were added to a flask, and the mixture was heated to 90 °C to form an optically clear solution. After cooling to room temperature, a total of 0.0228 g Na<sub>3</sub>PO<sub>4</sub>·12H<sub>2</sub>O was dissolved in 20 mL of water, and the solution was then injected into the flask under magnetic stirring. The reaction mixture was kept at 60 °C for 10 h and then kept at room temperature for 20 h. The as-taken solutions were precipitated with ethanol and isolated by centrifugation and decantation. The observed precipitate was dried under vacuum overnight to remove all solvents.

**Preparation of C-HA powders:** The conventional HA (C-HA) powders were from Biomaterials Center in Sichuan University. The powders were generally wet synthesized and spray dried with a SFDC-20 Spray Dryer (Shanghai Ohkawara Dryers Co., China). The as received powders were then sintered at 1100 °C for 2 h and then crushed and sifted through a 120-mesh (~125 μm) sieve.

**Preparation of Au nanoparticles:** Au nanoparticles were synthesized according to previous works.<sup>1</sup> In brief, HAuCl<sub>4</sub> (41 mg) and trisodium citrate solution (30 mg) were dissolved in water (38 mL), then 1 mL NaBH<sub>4</sub> (0.1 M) were rapidly injected to this mixture with vigorous stirring for 5 min at room temperature, and its color changed from pale

yellow to deep red. The resulting solution was filtered with a PTFE membrane (filter unit is 0.22  $\mu\text{m}$ ) to remove some large clusters and insoluble compounds.

**Preparation of Au@HA nanoparticles:** In a typical synthesis, 0.0607 g  $\text{Ca}(\text{SA})_2$ , 2.0 mL of OA, and 20.0 mL of toluene were added to a flask, and the mixture was heated to 90  $^\circ\text{C}$  to form an optically clear solution. After cooling to room temperature, a total of 0.0228 g  $\text{Na}_3\text{PO}_4 \cdot 12\text{H}_2\text{O}$  was dissolved in 20 mL of water, following which the as-prepared Au nanoparticles were added to the solution, and the solution was finally injected into the flask under magnetic stirring. The reaction mixture was kept at 60  $^\circ\text{C}$  for 10 h and then kept at room temperature for 20 h. As-taken solutions were precipitated with ethanol and isolated by centrifugation and decantation. The observed precipitate was dried under vacuum overnight to remove all solvents.

**Preparation of DOX@HA nanoparticles:** In a typical synthesis, 0.0607 g  $\text{Ca}(\text{SA})_2$ , 2.0 mL of OA, and 20.0 mL of toluene were added to a flask, and the mixture was heated to 90  $^\circ\text{C}$  to form an optically clear solution. After cooling to room temperature, a total of 0.0228 g  $\text{Na}_3\text{PO}_4 \cdot 12\text{H}_2\text{O}$  was dissolved in 20 mL of water, then 500  $\mu\text{L}$  DOX (0.001 M) aqueous solution was added, the solution was finally injected into the flask under magnetic stirring. The reaction mixture was kept at 60  $^\circ\text{C}$  for 10 h and then kept at room temperature for 20 h. As-taken solutions were precipitated with ethanol and isolated by centrifugation and decantation. The observed precipitate was dried under vacuum overnight to remove all solvents.

#### **Characterization of samples:**

The XRD patterns were obtained using a Dandong Fangyuan DX-1000 diffractometer (China) using  $\text{CuK}\alpha$  radiation ( $\lambda=1.5418 \text{ \AA}$ ) and employing a scanning speed of 0.02  $^\circ/\text{s}$  in the  $2\theta$  range 10 $^\circ$ - 80 $^\circ$ .

A field emission scanning electron microscope (SEM, S-4800, Japan), equipped with a Noran Voyager energy-dispersive spectroscopy (EDS) system was used for recording the SEM images and element distribution maps.

The TEM images were acquired using a transmission electron microscope (TecnaiG2F20S-TWIN, USA) at an accelerating voltage of 120 KV. Samples for TEM observation were prepared by dropping 10  $\mu\text{L}$  of diluted ethanol solution onto 400-mesh carbon-coated copper grids. The average particle size and distribution were determined by size distribution diagrams, which were quantified using ImageJ software from TEM pictures. The average particle shell thickness was also quantified similarly. HRTEM measurements were performed using a TEM system operated at an acceleration voltage of 200 KV.

The FTIR spectra were measured at room temperature with a Perkin-Elmer Spectrum one (B) (USA) spectrometer using KBr pellet technique.

Nitrogen adsorption-desorption isotherms were measured with an ASAP 2020 Micromeritics Instrument (USA) at 77 K. Before the measurement, the sample was degassed at 25  $^\circ\text{C}$  overnight. The specific area was calculated from the linear part of the Brunauer-Emmett-Teller (BET) equation ( $P/P_0 \approx 0.05-0.30$ ).

**Drug delivery test:** The delivery test was performed by immersing the DOX loaded hollow HA spheres (DOX@HA, 2 mg) in 10 mL PBS under gentle stirring under dark conditions, and the immersing temperature was kept at 37 °C. At selected time intervals, predetermined samples were centrifuged and immediately replaced with an equal volume of fresh PBS. The supernatant was analyzed by a fluorescence spectrophotometer, excited at 480 nm. Each experiment was carried out in triplicate. Hollow HA nanospheres loading DOX by adsorption was used as control to compare the drug release. The adsorbing-loaded sample was prepared as follow: hollow HA nanospheres (10 mg) were mixed with DOX solution (500  $\mu$ L, 0.001 M) in Na<sub>3</sub>PO<sub>4</sub> (20 mL). After stirring for 10 h under dark conditions, the adsorbed HA particles were centrifuged and washed with water. The particles were dried for subsequent tests of DOX release. Fluorescence spectra was recorded on a F-7000 spectrofluorometer (HITACHI, Japan).

**Protein adsorption to hollow HA nanospheres:** Bull serum protein (BSA) was used as a model protein to investigate the possibility of hollow HA nanospheres using as protein carrier by surface adsorption. For the quantification of protein adsorption onto the different latex dispersions, a BCA protein assay kit from Pierce (Rockford, IL) was used. Protein adsorption experiments were carried out in 1.5 mL low adsorption microcentrifuge tubes. Samples (1 mg) were equilibrated with 1 mL of protein solution, at a concentration for 0.25-1.0 mg/mL. After incubation at 37 °C for 2 h with continuous shaking, the mixtures were centrifuged for 5 min at 7,000 rpm and the supernatants were quantitatively assayed by the BCA method using absorbance values at a wavelength of 570 nm with a  $\mu$ Quant spectrophotometer (Bio-Tek Instruments Inc., USA) against water blank. The amounts of adsorbed protein on the particles were calculated from the mass balance. C-HA was used as control to compare the protein adsorption capacity of hollow HA nanospheres. All experiments were carried out in triplicate.

**Cell viability assay of hollow HA nanospheres:** The in vitro cell viability of hollow HA nanospheres compared to C-HA was evaluated by MG63 cell proliferation analysis. The cells ( $2 \times 10^4$  /well), seeded in 24-well plate, were co-cultured with two different materials as-prepared (30  $\mu$ g/mL), respectively, at 37 °C in a humidified atmosphere of 5 % CO<sub>2</sub>. Cells cultured in the medium without the addition of HA materials was used as control and all assays were performed in triplicate. After cultured for 1, 3, and 5 days, cells were incubated with 0.5 mg/mL MTT for 4 h at 37 °C. The solution was then removed and purple formazan salts dissolved with DMSO, and the absorbance of the resulting solution was measured at 490 nm using a multidetection microplate reader (Bio-Tek Instruments Inc., USA).

**Cellular uptake, imaging and cytotoxicity of DOX@HA :** MG63 cells were seeded at a concentration of  $1 \times 10^4$  cells/well with hollow HA nanospheres and DOX@HA (150  $\mu$ g/mL). After culturing for 1, 3 and 5 days, cells were washed two times with PBS and fixed in 4 % paraformaldehyde solution for 10 min. After rinsed in PBS, 0.1 % (v/v) DAPI solution was added to the samples to stain the nuclei following 10 min incubation at room temperature, after which the samples were washed two times in PBS for imaging by fluorescence microscope (Leica OMI4000B, Germany).

## 2. Supplementary experimental results and figures

### 2.1 The chemical constituents of the hollow HA nanospheres

FTIR analysis was carried out for confirming the functional groups presenting in the as-prepared hollow HA spheres, which in turn provided information about the constitution and phase composition of the products synthesized in two-phase system.

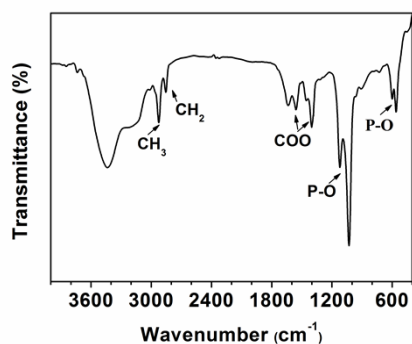


Fig. S1 FTIR spectrum of hollow HA spheres.

### 2.2 The change of atomic composition during the different stages of the reaction

Besides XRD structural characterization, EDS element analysis have been performed on the as-prepared nanocrystals.

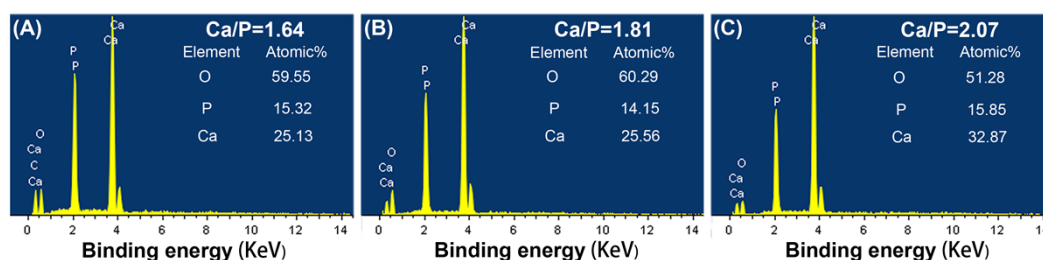


Fig. S2 EDS patterns of the products synthesized in 60 °C for (A) 10 h; (B) 5 h; (C) 30 min and aging for 20 h in room temperature.

### 2.3 The distribution of size and shell thickness of the hollow HA nanospheres

Image-Pro Plus (Ver 6.0, Media Cybernetics) was employed to analyze the size of the crystal from TEM micrographs. More than 150 individual crystals were measured for each sample to obtain their mean size and size distribution. In this same way, we measured the shell thickness of the samples.

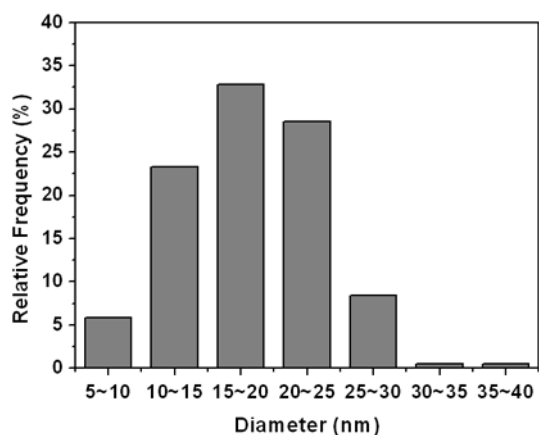


Fig. S3 Size distribution of the nanoparticles.

As shown in Fig. S3, statistical result showed that the size distribution of the hollow spheres in the typical conditions was in the range of 10-30 nm and the average shell thickness was  $5.4 \pm 1.6$  nm, which indicated the narrower size distribution.

#### 2.4 Specific surface area measurement

Using Nitrogen adsorption-desorption isotherm in Fig. S4, we calculated the specific surface area of  $138.8 \text{ m}^2/\text{g}$  from the linear part of the Brunauer-Emmett-Teller (BET) equation ( $P/P_0 \approx 0.05-0.30$ ).

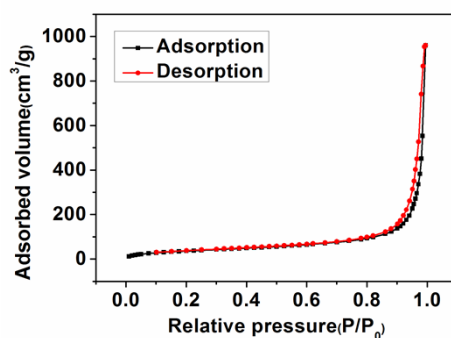


Fig. S4 Nitrogen adsorption-desorption isotherm of hollow HA nanospheres.

#### 2.5 Average structure of the HA facets from materials studio simulations

To further understand the growth process of the hollow HA spheres, we simulated atomic arrangement of different facets and calculated the related atom density. HA planar atom density  $D$  can be calculated as  $D=N/A$  (where  $N$  and  $A$  represent the numbers of the atoms of the HA facet and the area of the HA facet, respectively).<sup>2</sup> Fig. S5A shows the ball-and-stick models of three HA facets, and the planar density of  $\text{Ca}$ ,  $\text{PO}_4^{3-}$  and  $\text{OH}^-$  in three analyzed HA facets are listed in Fig. S5B.

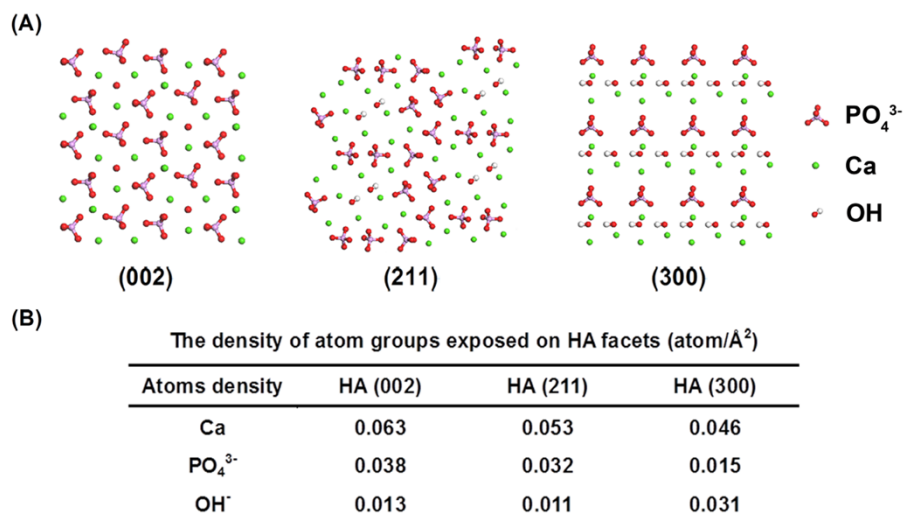


Fig. S5 (A) Ball-and-stick models of HA facets; (B) The density of atom groups exposed on HA facets.

## 2.6 Encapsulated Au@HA nanoparticle

In order to prove the possibility to create multifunctional materials by filling target materials into the cavities of the hollow HA spheres and allow a convincing check of the validity of the mechanistic assumptions, the inorganic nanoparticles (Au nanoparticles) encapsulation experiment was designed.

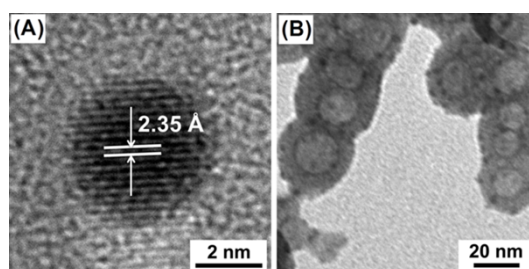


Fig. S6 (A) HRTEM image of Au nanoparticles; (B) TEM image of the products of Au@HA.

Fig. S6 shows the 2.35 Å spacing of (111) lattice spacing of Au inside the hollow spheres (Fig. S6A) and that Au nanoparticles were successfully incorporated into both the cavities and the shells of hollow HA nanospheres (Fig. S6B). These results clearly indicate that Au@HA nanostructures were formed in the two-phase system. The hollow nature together with the tunable interior core make them ideal entity for inter incorporation, which might bring novel optical, electronic and magnetic properties, depending on the properties of the incorporated nano particles.

## 2.7 Drug loading by encapsulation

To examine the drug loading and delivery ability of the hollow HA nanospheres, DOX, an anticancer drug, was loaded into hollow spheres in the process of the reaction to yield DOX encapsulated hollow HA nanospheres (DOX@HA).

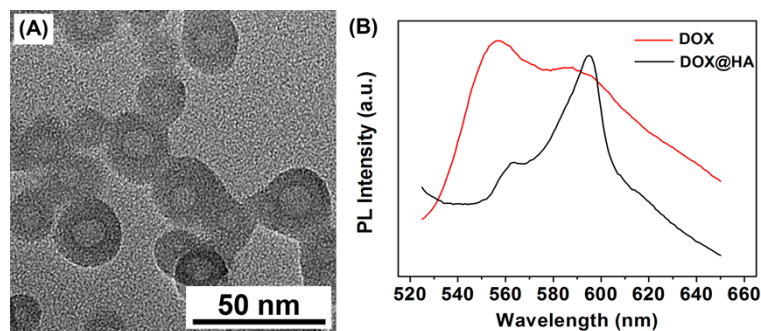


Fig. S7 (A) TEM image of DOX@HA spheres; (B) PL spectra of free DOX and DOX@HA spheres.

As shown in Fig. S7, DOX as water-soluble drug molecules can be successfully encapsulated into the cavities of hollow HA, and the hollow structure wouldn't be damaged by the drug storage process. Due to the interaction of DOX and hollow HA sphere during the reaction, the relative intensity had changed, combined with a little red shift. In order to verify the merits of the high drug loading capacity of hollow spheres, we designed adsorbing-loaded sample as a control, in which the DOX molecules were adsorbed onto the surface of hollow spheres.

## 2.8 Drug control release

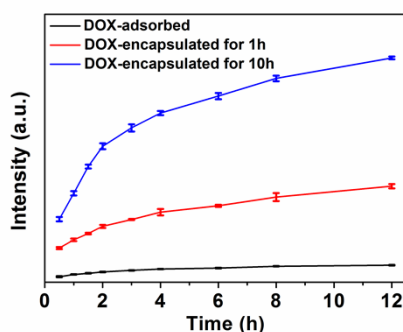


Fig. S8 Release profile of DOX from DOX@HA spheres (encapsulated for 1 h and 10 h respectively) in PBS (pH=5.0) at 37 °C.

Fig. S8 shows the release behavior of the drug from the capsules of DOX@HA spheres over a 12 h period in PBS (pH=5.0) at 37 °C. In comparison of relative strength, the amount of DOX encapsulated into the cavities is much higher than DOX adsorbing-loaded on the surface. In addition, the release of drug stored in the carrier can occur when the hollow shells were incubated in a relatively low pH value. The experimental results indicate that this kind of hollow HA spheres are very promising for drug loading and delivery.

## 2.9 Protein adsorption

The potential of hollow HA nanospheres using as protein carrier by surface adsorption was characterized by the testing of adsorbed BSA with BCA assay. C-HA was used as control.

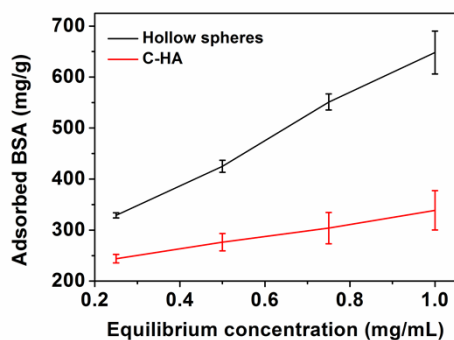


Fig. S9 Adsorption isotherms of BSA on the two types of HA powders.

It can be seen from Figure S9 that the hollow spheres showed significantly higher adsorption capacities than C-HA. This indicates that the hollow HA nanospheres can be better used as a carrier for proteins or drugs by surface adsorption compared to the conventional nanoparticles.

### 2.10 Cell viability of hollow HA nanospheres

One of the outstanding advantages of HA in biomedical applications is its good biocompatibility. Here, the MTT assay was implemented to compare the viability of MG63 cells on both hollow HA nanospheres and C-HA, as well as the control.

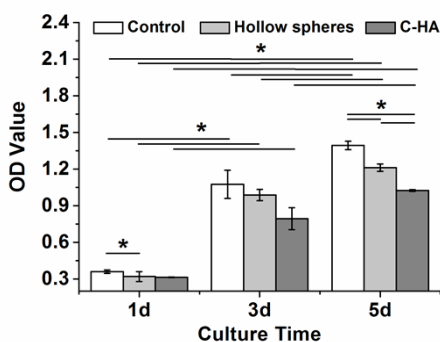


Fig. S10 MTT analysis of the MG63 cells cultured with different HA after 1, 3, 5 days (\* $p < 0.05$ ).

As Fig. S10 shown, MG63 cells in all the three groups show good proliferation with incubation time, although the cell viability of the both material groups is a little lower than that of the control. It is worthy to note that in comparison with C-HA, cells cultured with hollow HA spheres show higher viability. Basing on the well-known excellent biocompatibility of C-HA and the results here, it can be concluded that the hollow HA nanospheres have good biocompatibility.

### 2.11 Cellular uptake, imaging and cytotoxicity of DOX@HA

The proliferation, distribution, and morphology of MG63 cells cultured with hollow HA nanospheres and DOX@HA was visualized with a fluorescence microscope as shown in Fig. S11.



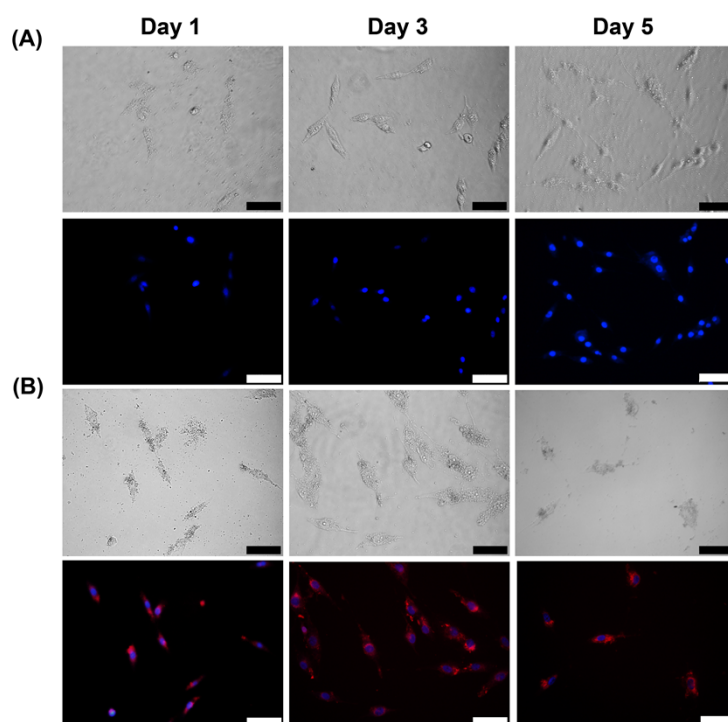


Fig. S11 Light micrographs and fluorescent microscope image of cells (A) hollow HA and (B) DOX@HA after 1, 3, 5 days. Scale bars: 100  $\mu\text{m}$ .

The red staining of cells cultured with DOX@HA indicates that the nanospheres can be uptaken by cells and hollow HA nanospheres can help carry the DOX into cells. From day 1 to day 5, MG63 cells cultured with hollow HA nanospheres maintained a steady proliferation and eventually developed a typical spindle shape, indicating the cytocompatible and non-toxic nature of hollow HA nanospheres. In contrast, cells showed a tendency of apoptosis after culturing with DOX@HA for 5 days, expressing in the significantly decreased cell number and indistinct cell boundary. It indicates that through the method water-soluble drugs can be loaded onto the hollow spheres, which can enter cells, gradually release and achieve therapeutic effect.

## References

- 1 G. S. Métraux and C. A. Mirkin, *Advanced Materials*, 2005, **17**, 412.
- 2 H.-p. Zhang, X. Lu, Y. Leng, L. Fang, S. Qu, B. Feng, J. Weng and J. Wang, *Acta biomaterialia*, 2009, **5**, 1169.